Journal of Ceramic Processing Research. Vol. 17, No. 2, pp. 80~84 (2016)

J O U R N A L O F
Ceramic Processing Research

Optical and electrical properties of SnO_2/Ag/ SnO_2/SiO_2/Nb_2O_5 hybrid film

Jin-Gyun Kim, Sang-Moo Yoon and Gun-Eik Jang*
Department of Materials Engineering, Chungbuk National University, Cheongju, 362-763, Korea

A hybrid structure of SnO_2/Ag/SnO_2/SiO_2/Nb_2O_5 was deposited on soda lime glass substrate by sequential RF/DC magnetron sputtering at room temperature and its optical and electrical properties were systematically investigated as a function of top SnO_2 thickness. EMP simulation results suggested that a multilayered film of SnO_2 (40 nm)/Ag (10 nm)/SnO_2 (30 nm)/SiO_2 (10 nm)/Nb_2O_5 (10 nm) exhibited the highest visible transmittance of 90.1% at 550 nm, whereas experimentally measured transmittance showed 85.1%, somewhat lower than simulation data. The lowest R_s and ρ value were about 3.21 Ω/sq and 3.21 × 10^{-5} Ω cm, acquired at the multi-layers with the structure of SnO_2 (40 nm)/Ag (10 nm)/SnO_2 (30 nm)/SiO_2 (10 nm)/Nb_2O_5 (10 nm). In addition, the sheet resistance and resistivity of SnO_2/Ag/SnO_2/SiO_2/Nb_2O_5 multi layer films increased systematically with increasing the thickness of SnO_2 layer from 40 to 55 nm. It was shown that the Ö$_{TC}$ values of SnO_2/Ag/SnO_2/SiO_2/Nb_2O_5 multi layer film were in the range of 46.4-62.1 × 10^{-3} Ω^{-1}.

Key words: TMT structure, Transmittance, Sheet resistance, Φ_{TC}.

Introduction

Transparent conducting electrodes (TCEs) are of great technological importance for a wide variety of applications in optoelectronic, photovoltaic devices and systems such as solar cell, organic light emitting diodes, and liquid crystal displays [1, 2]. So far, a number of research projects have been successfully conducted in the area of tanspatarent conducting oxide (TCO) materials [3-8]. Recently, many researchers proposed TCO/metal/TCO (TMT) tri layer structures with much low resistance as good candidates for TCEs. Serveral advantages of TMT tri layer structures have been reported, which have include low sheet resistance, high optical transparency in the visible range and relatively better chemical stability than single-layered metal film [9-15].

Among many commercial applications using TCO material, touch screens in particular, are becoming increasingly popular because of their ease and versatility of operation as well as their cost effectiveness. However, when the touch sensor panel in touch screens composed with TCO and adhesive is used in a bright environment, incident light can hit the interfaces between those layers of the stackup having mismatched refractive indices and can reflect off those interfaces. The light reflected from those interfaces can give rise to the appearance of fringes on the touch sensor panel, which can be visually distracting. In order to reduce the fringe effect, reflectance change at the interface, by placing the index matching layer with high and low refractive index materials into layers of the stackup, could be one of possible solutions in TMT structure. It was already known that the presence of an index matching layer can reduce the amount of reflection between the adbesive-ITO interface, which in turn, can reduce the interference of reflected light and the appearance of fringes on the touch sensor panel [16-17]. However, not many systematic works have been undertaken to study the modification of optical properties through the addition of index matching layers into tri-layer structure.

In the present study, a hybrid structure of SnO_2/Ag/ SnO_2 film with an index matching layer has been designed. As index matching materials, SiO_2 (n = 1.46) and Nb_2O_5 (n = 2.34) with low and high refractive indices, which have been the most successful application in electronic industry as electrical contact, were selected for this purpose. The objective of present research is to evaluate the optical and electrical characteristics of SnO_2/Ag/SnO_2/SiO_2/Nb_2O_5 multilayer film with different top layer of SnO_2 thickness. In order to estimate the optical characteristics and compare them with experimental results in advance, the simulation program named EMP (Essential Macleod Program) was adopted.

Experimental

Simulation

Prior to the experiments, one of the optical programs named Essential Macleod Program (EMP) was used to simulate the optical characteristics such as transmittance, reflectance and color in the multi layer thin films. The EMP was processed through the following steps; first, construction parameters such as reflectance and extinction

*Corresponding author:
Tel : +82-43-261-2412
Fax: +82-43-271-3222
E-mail: gejang@chungbuk.ac.kr

coefficient of SnO_2, Ag, SiO_2 and Nb_2O_5, respectively, which were calculated by ellipsometry measurement, were input in the program. Second, SnO_2/Ag/SnO_2/SiO_2/Nb_2O_5 multi layers were designed and simulated with various parameters such as wavelength ranges (380-780 nm), thickness (10-55 nm), stacking sequence and layers of structure. Finally, analysis on the parameter effect was performed with system modification for optical properties whether it is appropriated for the optimum simulation.

Film preparation

For the purpose of study, SnO_2 (40-55 nm)/Ag (10 nm)/SnO_2 (30 nm)/SiO_2 (10 nm)/Nb_2O_5 (10 nm) multi layer film with more than about 85% transmittance was selected after taking a number of simulation by modifying the stacking sequence and adjusting the thickness of each layer. Fig. 1 shows a schematic diagram illustrating the structure of SnO_2/Ag/SnO_2/SiO_2/Nb_2O_5 multi layer film. A hybrid structure of SnO_2/Ag/SnO_2/SiO_2/Nb_2O_5 was deposited on soda lime glass substrate by sequential RF/DC magnetron sputtering at room temperature. Prior to deposition, soda-lime glass ($75 \times 25 \times 1$ mm^3) was ultrasonically cleaned in acetone, ethanol and IPA for 30 min at 50 ºC. Thin film layers of SnO_2, SiO_2, and Nb_2O_5 were deposited by RF magnetron sputtering onto soda-lime glass substrates at room temperature. High purity Ar (35 sccm) was introduced into the chamber by mass flow meter with the total pressure maintained at 5.5 mTorr. Ag layer was deposited by DC magnetron sputtering. The total film thickness was about 100 nm. The thickness of each layer was controlled by increase the sputtering time at constant optimized conditions. More details about sputtering conditions are given in Table 1. The refractive index n and extinction coefficient k of each monolayer were evaluated using ellipsometer (Elli-SE) in the visible range from 350 to 750 nm with a step with of 5 nm. Crystalline structures and phase identification of the multi layer film were characterized by X-ray diffractometer. The micro-structural examination and surface roughness of the films was investigated by Field emission electron microscopy (LEO-1530) and Atomic Force Microscope (AFM) measurements in contact mode. Transmittance and reflectance of the films were estimated using a UV-VIS-NIR spectrophotometer (KONICA-MINOLTA CM-3600d) with a light source of D65. In addition, the interfacial properties of SnO_2/Ag/SnO_2/SiO_2/Nb_2O_5 electrodes were analyzed using AES depth profiling. The sheet resistance was detected by a four-point probe system.

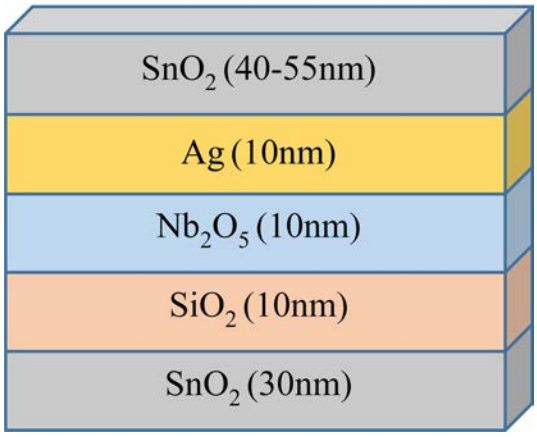

Fig. 1. A schematic diagram illustrating the structure of SnO_2/Ag/SnO_2/SiO_2/Nb_2O_5 multi layer film.

Table 1. Deposition parameters and sputtering condition of SnO_2/Ag/SnO_2/SiO_2/Nb_2O_5 multi layer film.

Parameter	Condition	
Sputtering	RF	DC
Target	SiO_2, Nb_2O_5, SnO_2	Ag
Substrate	Glass	
Power	100 W	10 W
Base pressure	5×10^{-5} Torr	
Working pressure	1.1×10^{-3} Torr	
Temperature	R.T.	
Atmosphere (Ar)	35 sccm	

Results and Discussion

Optical properties

To extract an accurate analysis from EMP simulation, the refractive index n and extinction coefficient k are necessary. The obtained refractive indices of SiO_2, Nb_2O_5, SnO_2 and Ag thin films were 1.52, 2.42, 2.09 and 0.12, respectively, which are somewhat higher than theoretical value. The slightly high value of n is thought to arise from low density and low crystallinity of each film owing to their low processing temperature. Further, the measured extinction coefficients of SiO_2, Nb_2O_5, SnO_2 and Ag are 0.02, 0.0, 0.0 and 2.98, respectively. Table 2 shows comparison of the refractive index n and extinction coefficient k with theoretical and experimental data, respectively.

Prior to experiments, the optical programs named Essential Macleod Program (EMP) was carried out to simulate the optical characteristics. Based on results from a number of simulations, the film thickness of the

Table 2. Comparison of the refractive index n and extinction coefficient k with theoretical and experimental data.

Materials	Theoretical value		Experimental value	
	n	k	n	k
SiO_2	1.46	0	1.52	0.02
Nb_2O_5	2.34	0	2.42	0
SnO_2	2.04	0	2.09	0
Ag	0.15	3.47	0.12	2.98

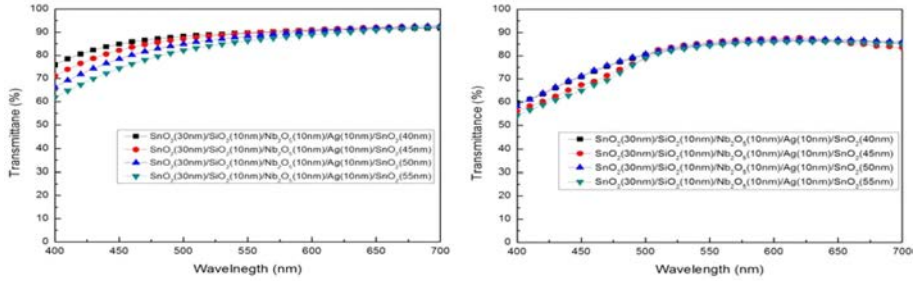

Fig. 2. (a) Simulated and (b) experimentally measured optical transmittance spectra on the SnO_2/Ag/SnO_2/SiO_2/Nb_2O_5 multi layer film as a function of thickness of the top SnO_2 layer.

top SnO_2 layer were varied from 40 to 55 nm, whereas SiO_2, Nb_2O_5 and Ag layers were fixed at 10 nm and the bottom SnO_2 layer was kept at 30 nm. Fig. 2(a) exhibited the optical simulation spectra of transmittance on SnO_2 (40-55 nm)/Ag (10 nm)/SnO_2 (30 nm)/SiO_2 (10 nm)/Nb_2O_5 (10 nm) multi layer film as a function of the top layer thickness of SnO_2. As can be seen from simulation spectra of Fig. 2(a), transmittance of the most films shows sharp transmittance increase in the visible region. However, transmittance gradually decreased from 90.1% to 86.7% at 550 nm wavelength with increasing the top SnO_2 thickness from 40 to 55 nm. Fig. 2(b) shows the experimentally measured transmittance taken from the same multilayer films as a function of the top SnO_2 thickness. As compared with that obtained through simulation, transparencies obtained from experimental spectra were slightly varied from 84.3% to 85.1% at 550 nm, and transmittance becomes gradually lowered. This might be attributed to light scattering on the each layer of film surface and interface instability due to elemental diffusion. Moreover, the substrate temperature processed room temperature was also considered to cause crystalliny difference of each layer between the experimental and EMP simulation results.

Phase identification and surface morphology analysis

Crystalline structures of the multi layer film were characterized by X-ray diffractometer. XRD spectra of SnO_2 (40-55 nm)/Ag (10 nm)/SnO_2 (30 nm)/SiO_2 (10 nm)/Nb_2O_5 (10 nm) coated multi layer films as a function of SnO_2 top layer thickness are shown in Fig. 3. It can be seen in Fig. 3 that all the as-deposited multi layer films appear to be amorphous regardless of SnO_2 thickness. There was a broad diffraction peak at 26 ° for all samples that is caused mainly by the glass substrate. This can be explained that thin film with about 100 nm thick has a nanocrystalline phase formed during DC/RF sputtering process. In addition, weak Ag (111) peaks could be detected around 38.3 ° in SnO_2/SiO_2/Nb_2O_5 multi layer film with 10 nm thickness of Ag layer. Fig. 4 represents AFM images of SnO_2/Ag/SnO_2/SiO_2/Nb_2O_5 multi layer film as a function of the thickness of top SnO_2 layer. As can be seen in Fig. 4, the

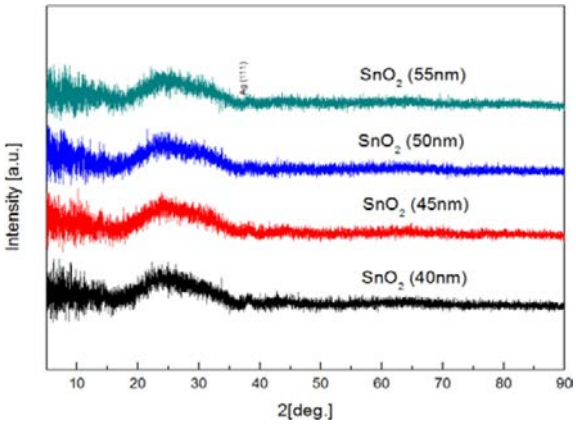

Fig. 3. XRD patterns obtained from SnO_2 (40-55 nm)/Ag (10 nm)/SnO_2 (30 nm)/SiO_2 (10 nm)/Nb_2O_5 (10 nm) multi layer film with various SnO_2 layer thickness.

surface roughnesses are very smooth and maintained relatively small in the range of around 0.6 nm. AES depth profile of SnO_2 (40 nm)/Ag (10 nm)/SnO_2 (30 nm)/SiO_2 (10 nm)/Nb_2O_5 (10 nm) multi layer film was demonstrates in Fig. 5. All the peaks in the spectra can be accounted for by Sn, Ag, Si, Nb and O, the components of the film, respectively. The depth profiling spectra shown in Fig. 5 seems to show that interface between each layers was relatively well defined, especially interface between Sn and Ag electrode. However, it was found that Nb fractions are diffuse within the explored depth of Si and oxygen element was clearly observed on the silver matrix. One possible explanation is that there was a possible interfacial reaction between layers and thereby, element of the each layer has diffused into the film during processing

Electrical properties analysis

The variation in sheet resistance (R_s) and resistivity (ρ) of the coated multi layers as a function of SnO_2 layer thickness are displayed in Fig. 6. The measured resistance of the multi layers, R_s, can be defined as a function of the resistance of the single layers coupled in parallel, as described in the following equation [18]:

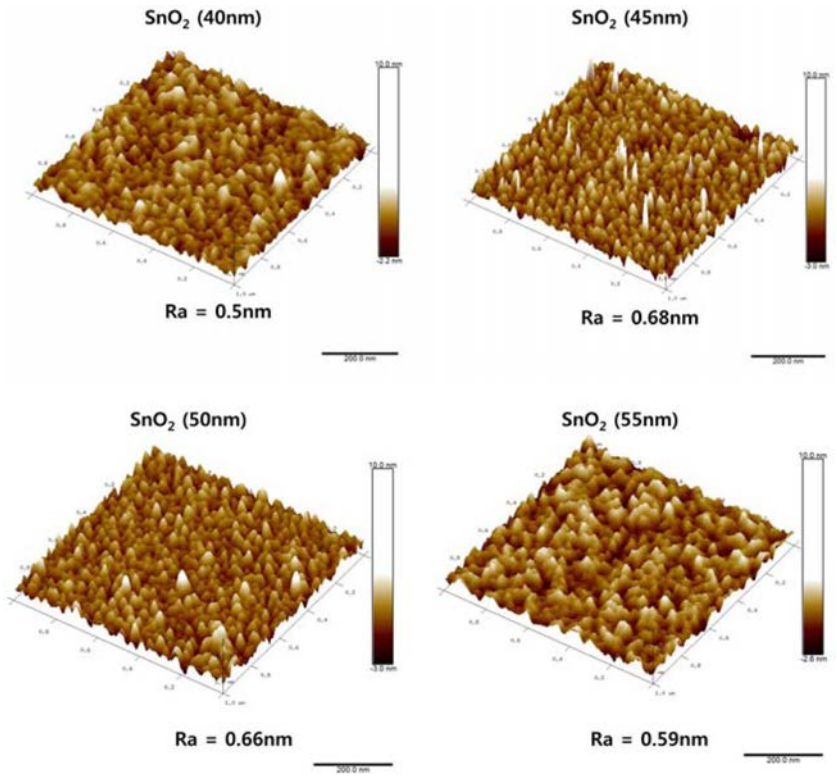

Fig. 4. AFM images of SnO_2/Ag/SnO_2/SiO_2/Nb_2O_5 multilayer films as a function of thickness of the top SnO_2 layer.

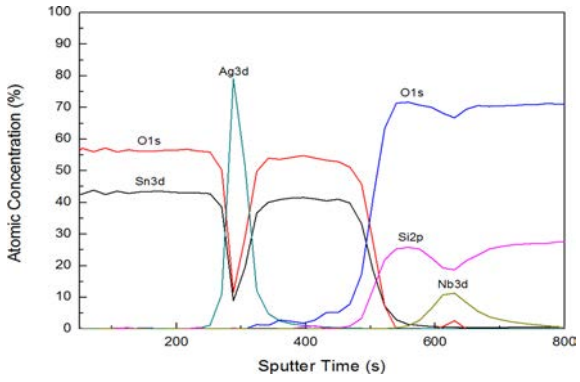

Fig. 5. AES depth profile of SnO_2 (40 nm)/Ag (10 nm)/SnO_2 (30 nm)/SiO_2 (10 nm)/Nb_2O_5 (10 nm) multi layer film.

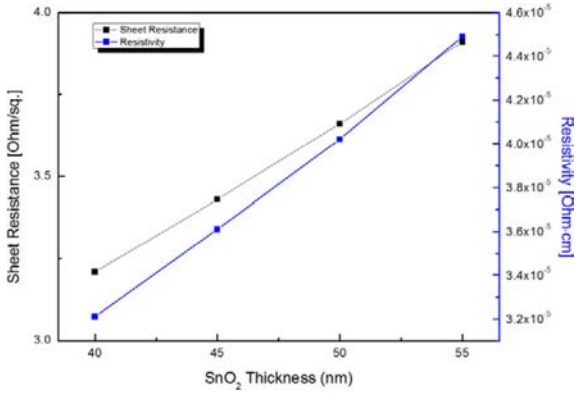

Fig. 6. The variation in sheet resistance (R_s) and resistivity (ρ) of SnO_2/Ag/SnO_2/SiO_2/Nb_2O_5 coated multi layers as a function of top SnO_2 layer thickness.

$$\frac{1}{R_S} = \frac{1}{R_{SnO_2top}} + \frac{1}{R_{Ag}} + \frac{1}{R_{SnO_2bottom}} + \frac{1}{R_{SiO_2}} + \frac{1}{R_{Nb_2O_5}} \quad (1)$$

Where R_s is sheet resistance of the multi layers, R_{SnO_2top}, R_{Ag}, R_{SnO_2bot}, R_{SiO_2} and $R_{Nb_2O_5}$ are sheet resistance of top SnO_2, Ag, bottom SnO_2, SiO_2, and Nb_2O_5, respectively.

As can be seen from Fig. 6, the lowest Rs and ñ value were about 3.21 Ω/sq and 3.21×10^{-5} Ω cm, acquired at the multi-layer with the structure of SnO_2 (40 nm)/Ag (10 nm)/SnO_2 (30 nm)/SiO_2 (10 nm)/Nb_2O_5 (10 nm). Moreover, the sheet resistance and resistivity of the SnO_2/Ag/SnO_2/SiO_2/Nb_2O_5 multi layer films increased systematically with increasing thickness of top SnO_2 layer from 40 to 55 nm. Generally, it was known that the total resistivity of the trilayers is mainly determined by Ag layer [14]. However, in this study, the sheet resistance was varied as a function of top SnO_2 layer thickness. In TCO applications, optimization the coating parameter lays a key role on electric and optical characteristics. The figure of merit (Φ_{TC}), commonly derived by Haacke [19], is an important factor that represents the relationships between sheet resistance and optical transmittance.

Fig. 7 demonstrated the calculated Φ_{TC} with increasing the top SnO_2 layers. It was shown that the Φ_{TC} values of SnO_2/Ag/SnO_2/SiO_2/Nb_2O_5 multi layer film were in the range of 46.4-62.1 $\times 10^{-3}$ Ω^{-1}. It is noted that SnO_2/Ag/SnO_2/SiO_2/Nb_2O_5 multi layer with 55 nm of SnO_2

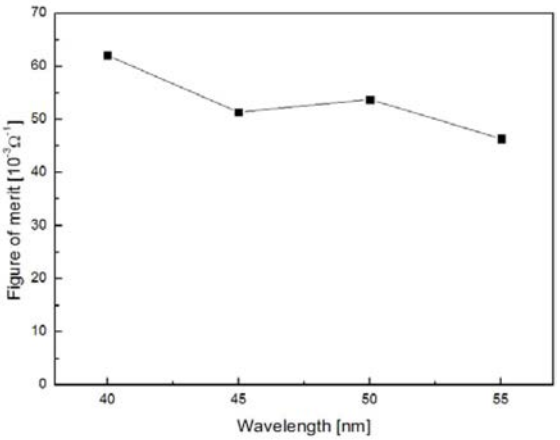

Fig. 7. The calculated Φ_{TC} with increasing the top SnO_2 layers in $SnO_2/Ag/SnO_2/SiO_2/Nb_2O_5$ multi layer film.

thickness resulted in a decrease of Φ_{TC} due to decrease of transmittance. The highest Φ_{TC} value ($62.1 \times 10^{-3}\ \Omega^{-1}$) of $SnO_2/Ag/SnO_2/SiO_2/Nb_2O_5$ film was obtained at a top SnO_2 thickness of 40 nm.

Conclusions

In summary, characteristics of the RF/DC sputtering grown hybrid structure of $SnO_2/Ag/SnO_2/SiO_2/Nb_2O_5$ with varying the SnO_2 thicknesses were systematically investigated. The transmittances were dependent on SnO_2 thickness. The measured transmittance suggested that a multi layer film of SnO_2 (45 nm)/Ag (10 nm)/ SnO_2 (30 nm)/SiO_2 (10 nm)/Nb_2O_5 (10 nm) exhibited high transmittance of 85.1% at 550 nm. XRD patterns obtained from SnO_2 /Ag /SnO_2 /SiO_2 /Nb_2O_5 multi layer film appear to be amorphous. The depth profiling spectra show that interface between each layer was relatively well defined. However, Nb fraction was diffused within the explored depth layer, indicating there was a possible interfacial reaction between Si and Nb layers. The lowest R_s and ñ value were about 3.21 Ω/sq and 3.21×10^{-5} Ω cm, acquired at a multi-layers with the structure of SnO_2 (40 nm)/Ag (10 nm)/SnO_2 (30 nm)/SiO_2 (10 nm)/Nb_2O_5 (10 nm). However, the sheet resistance and resistivity of $SnO_2/Ag/SnO_2/SiO_2/Nb_2O_5$ multi layer films increased systematically with increasing thickness of top SnO_2 layer from 40 to 55 nm. It is noted that $SnO_2/Ag/SnO_2/SiO_2/Nb_2O_5$ multi layer with 55 nm of SnO_2 thickness resulted in a decrease of Φ_{TC} due to decrease of transmittance. The highest Φ_{TC} value ($62.1 \times 10^{-3}\ \Omega^{-1}$) of $SnO_2/Ag/SnO_2/SiO_2/Nb_2O_5$ film was obtained at a top SnO_2 thickness of 40 nm.

Acknowledgments

This work was supported by Industrial Technology Innovation Program funded by the Ministry of Trade, Industry and Energy (MOTIE, Korea) (No. 10040000-10048659).

References

1. Podlogar M, Richardson JJ, Vengust D, Daneu N, Samadzjja Z, Bernik S, Recnik, Advanced Functional Materials, 22 (2012) 3136-3145.
2. R. Lachaume, W. Favre, P. Scheiblin, X. Garros, N. Nguyen, J. coignus, D. Munoz, G. Reimbold, Energy Procedia, 38 (2013) 770-776.
3. L. Liu, S. Mam, H. Wu, B. Zhu, H. Yang, J. Tang, X. Zhao, Materials Letters, 149 (2015) 43-46.
4. Q. Wan, E.N. Dattoli, W. Lu, Applied Physics. Letters, 90 (2007) 222107.
5. S. Yu, W. Zhang, L. Li, D. Xu, H. Dong, Y. Jin, Thin Solid Films, 552 (2013) 150-154.
6. H.J. Kim, K.W. Seo, Y.H. Kim, J.Y. Choi, H.K. Kim, Applied Surface Science, 328 (2014) 215-221.
7. D.R. Sahu, S.Y. Lin, J.L. Huang, Applied Surface Science, 252 (2006) 7509-7514.
8. A.E. Hajj, B. Lucas, M. Chakaroun, R. Antony, B. Ratier, M. Aldissi, Thin Solid Films, 520 (2012) 4666-4668.
9. X. He, W. Wang, S. Li, Y. Liu, W. Zheng, Q. Shi, X. Luo, Vacuum, 120 (2015) 17-21.
10. J.H. Kim, J.H. Lee, S.W. Kim, Y.Z. Yoo, T.Y. Seong, Ceramic International, 41 (2015) 7146-7150.
11. S.X. Zhang, S. Dhar, W. Yu, H. Xu, S.B. Ogale, T. Vendatesan, Applied Physics Letters, 91 (2007) 112113.
12. J.H. Kim, H.K. Lee, J.Y. Na, S.K. Kim, Y.Z. Yoo, T.Y. Seong, Ceramic International, 41 (2015) 8059-8063.
13. D. Miao, S. Jiang, S. Shang, Z. Chen, Vacuum, 106 (2014) 1-4.
14. D. Miao, S. Jiang, S. Shang, Z. Chen, Ceramics International, 40 (2014) 12847-12853.
15. A. Dhar, T.L. Alford, Journal of Applied Physics, 112 (2012) 103113.
16. C. Tung, E. Dorjgotov M. Kuwabara, S. Kang, C. Chen, J.Z. Zhong, *US Patent Application* 20150316689 A1 (2015).
17. L. Huang, S.C. Chang, N. Oldham, S.P. Hotelling, J. Z. Zhong, C.H. Tung, *US Patent Application* 20100141608 A1 (2010).
18. S. Venkatachalam, H. Nanjo, K. Kawasaki, Y. Wakui, H. Hayashi, T. Ebina, Applied Surface Science, 257 (2011) 8923-8928.
19. G. Haacke, Journal of Applied physics, 46 (1976) 4086.